Progress in Organic Coatings 150 (2021) 105989

Contents lists available at ScienceDirect

Progress in Organic Coatings

journal homepage: www.elsevier.com/locate/porgcoat

Green nanocomposites from Salvia-based waterborne polyurethane-urea dispersions reinforced with nanocellulose

Arantzazu Santamaria-Echart [a,b,*], Isabel Fernandes [b], Lorena Ugarte [a], Filomena Barreiro [b], Maria Angeles Corcuera [a], Arantxa Eceiza [a]

[a] Group 'Materials + Technologies', Department of Chemical and Environmental Engineering, Faculty of Engineering of Gipuzkoa, University of the Basque Country, Pza Europa 1, 20018 Donostia-San Sebastián, Spain

[b] Centro de Investigação de Montanha (CIMO), Instituto Politécnico de Bragança, Campus de Santa Apolónia, Bragança, 5300-253, Portugal

ARTICLE INFO

Keywords:
Waterborne polyurethane-urea
Cellulose nanocrystals
Salvia extract
Thermomechanical properties
Morphology

ABSTRACT

Waterborne polyurethane-urea (WBPUU) dispersions, products having none or low contents of organic solvents, depending on the used synthesis process, can provide suitable environmentally-friendly strategies to prepare novel materials. Moreover, waterborne systems enable the incorporation of aqueous dispersible nanoentities and soluble additives, which provides a strategy to design versatile functional materials with tailored properties. Having demonstrated in previous work the bacteriostatic properties of a 3 wt% Salvia-based WBPUU against *Staphylococcus aureus*, *Escherichia coli* and *Pseudomonas aeruginosa*, this work is focused in the preparation of Salvia-based WBPUU added with cellulose nanocrystals (CNC) tackling the preparation of functional green nanocomposite films with increased mechanical properties. Through this strategy, nanocomposites loaded with 1, 3 and 5 wt% of CNC were prepared, showing an effective CNC incorporation avoiding agglomerates. CNC addition is able to modulate soft and hard phase's segregation, inducing enhanced mechanical stiffness, together with improved deformability, while retarding thermomechanical instability to higher temperatures.

1. Introduction

Waterborne systems, particularly waterborne polyurethane-urea (WBPUU) dispersions, have drawn attention due to their versatility in terms of properties, which can be explored for different applications presenting advantages over the conventional solventborne systems [1]. The use of water to substitute organic solvents implies a reduction in the content of volatile organic compounds resulting in suitable alternatives to develop environmentally friendly products [2]. Moreover, dispersion's low-cost and scale-up potential, and characteristics such as high solids content, are among the benefits that avail their advantages to be applied in diverse applications [3–5]. Among WBPUU attractive characteristics, it is worth noting the advantages of their waterborne character, which facilitates the incorporation of nanoentities, either dispersible nanoreinforcements [6] or soluble additives, namely of natural origin [7,8].

Regarding natural additives, in a previous work [9] it was shown the suitability of incorporating natural extracts derived from plants as a strategy to impart functional properties to the WBPUU. The work specifically demonstrated that *Salvia officinalis* extracts, recognized for their antibacterial and antioxidant properties [10], were able to transferred these properties to the base WBPUU. Namely, the effect was positive against Gram-positive *Staphylococcus aureus*, and Gram-negative *Escherichia coli* and *Pseudomonas aeruginosa* bacteria.

The use of renewable nanoentities as nanoreinforcements, e.g. cellulose nanocrystals (CNC), can provide a strategy to enhance and modulate WBPUU polymer matrix properties. Among others, cellulose, the most abundant polysaccharide in the world, is biocompatible, biodegradable and presents low-toxicity [11]. The isolation of the crystalline domains of cellulose by removing the amorphous domains, leads to the obtainment of high length/diameter (L/D) aspect ratio CNC providing high stiffness nanoreinforcements [12].

In previous works, it has been corroborated the ability of CNC to tailor the properties of materials based on waterborne polyurethane dispersions, by analyzing CNCs incorporation route [13], or their effect in polyurethane microstructure [14], including the preparation of films

* Corresponding author at: Group 'Materials + Technologies', Department of Chemical and Environmental Engineering, Faculty of Engineering of Gipuzkoa, University of the Basque Country, Pza Europa 1, 20018 Donostia-San Sebastián, Spain.

E-mail addresses: asantamaria@ipb.pt (A. Santamaria-Echart), ipmf@ipb.pt (I. Fernandes), lorena.ugarte@ehu.eus (L. Ugarte), barreiro@ipb.pt (F. Barreiro), marian.corcuera@ehu.eus (M.A. Corcuera), arantxa.eceiza@ehu.eus (A. Eceiza).

https://doi.org/10.1016/j.porgcoat.2020.105989
Received 4 June 2020; Received in revised form 3 September 2020; Accepted 5 October 2020
Available online 14 October 2020

[15] and mats [16]. The incorporation to polyurethane-urea dispersions was also studied [17] using a chemical system where a short chain diol was included in the pre-polymer preparation, before the final chain extension with a diamine. In this work, properties modulation of CNCs was studied with a Salvia-based polyurethane-urea system using only the amine extension reaction. Apart from the conferred functional properties to the matrix, Salvia extract can provide a surfactant effect, being a co-adjuvant facilitating the synthesis and stability of the WBPUU [18,19].

In this context, this work is focused on the preparation of green nanocomposites from a Salvia-based WBPUU used as matrix. For that, isolation and incorporation of CNC were studied. The selected Salvia-based WBPUU comprised a load of 3 wt% of the respective aqueous extract, which was incorporated following an *in-situ* strategy, i.e. the incorporation was made during the dispersion formation step. This selection followed previous results that pointed out this formulation as the most promising based on its stability and bacteriostatic effects. To enhance the mechanical properties of the produced nanocomposites, Salvia-loaded WBPUU were modified with different contents of CNC (1, 3, and 5%), and thereafter used in the preparation of the films. The prepared films were characterized in terms of physicochemical, thermal, mechanical, and thermomechanical properties. Moreover, in order to corroborate the successful addition of CNC and their properties modulating effects, morphology studies of the nanocomposite films were conducted.

2. Experimental

2.1. Materials

CNC were obtained from microcrystalline cellulose (MCC) powder purchased from Aldrich using concentrated sulfuric acid (H_2SO_4) provided from Panreac.

The synthesis of Salvia-based WBPUU was carried out using poly (ε-caprolactone)diol (PCL) ($\overline{M}_w$ =2000 g/mol) provided by Solvay as the soft segment (SS), previously dried under vacuum at 50 °C for 4 h. The hard segment (HS) was composed by isophorone diisocyanate (IPDI), kindly purchased from Covestro, as the isocyanate component, ethylenediamine (EDA), supplied by Panreac, as the chain extender, and 2,2-bis(hydroxymethyl)propionic acid (DMPA), purchased from Fluka, as the internal emulsifier. DMPA was dried at 50 °C for 4 h under vacuum before use. DMPA acid groups were neutralized with triethylamine (TEA), provided by Fluka. Dibutyltin dilaurate (DBTDL), supplied by Fluka, was used as the catalyst. Dry acetone, supplied by Panreac, was used to adjust the viscosity during the synthesis process. Salvia officinalis L. from Raizes da Natureza was acquired in a local herbalist.

2.2. Isolation of cellulose nanocrystals

Cellulose nanocrystals were isolated by removing the amorphous region of MCC by acid hydrolysis with H_2SO_4 according to a previously developed methodology [13]. Briefly, MCC was mixed with H_2SO_4 (64 wt%) at 45 °C for 30 min and then diluted with deionized water. The resultant suspension was washed by using centrifugation cycles and dialyzed to obtain a final CNC suspension with a pH of about 5–6 and a solids content of 0.5 wt%.

2.3. Preparation of the Salvia-based WBPUU

The synthesis of the Salvia-based WBPUU dispersion, with a hard segment content of 32 wt%, was carried out by a two-step polymerization process, using a 5 wt% DMPA content and an NCO/OH molar ratio of 1.67 in the prepolymer synthesis step. Salvia extract (pH 5.52) was incorporated at 3 wt% based on the total WBPUU dry weight. For the reaction, a 500 mL four-necked jacketed reactor equipped with a thermocouple, a mechanical stirrer and an intracooler, was employed. The reaction progress (under nitrogen atmosphere), was assured by the dibutylamine back titration method, according to the ASTM D 2572-97. In the first step, PCL and IPDI were reacted at 80 °C in the presence of 0.037 wt% of DBTDL until the theoretical NCO value was reached. Then, DMPA (previously neutralized with TEA in acetone solution) was incorporated and let to react at 50 °C. Afterwards, the NCO terminated prepolymer was cooled to 25 °C for the phase inversion. In this step, Salvia extract, obtained according to the infusion method as previously described [9], was dissolved in the required amount of distilled water, and then added dropwise under vigorous stirring to the pre-polymer reactive mixture. The obtained dispersion was heated to 35 °C, and the chain extender, EDA dissolved in 20 mL of distilled water (added amount based on a chain extension degree of 40 %), added at a flow rate of 0.3 mL/min. The acetone was removed in a rotary evaporator (40 °C and 350 mbar), leading to a product exempt (or with only traces) of organic solvents.

2.4. Nanocomposite films preparation

Salvia-based WBPUU dispersion was employed as the matrix for the preparation of the nanocomposites containing CNC (from 0 to 5 wt%). In a first step, a CNC suspension (pH 5-6) was sonicated for 1 h and thereafter incorporated into the Salvia-based WBPUU dispersion (1.55, 4.77 and 8.12 g of CNC suspension to prepare the nanocomposites with 1, 3 and 5 wt% of cellulose nanocrystals, respectively). The resultant mixture was sonicated for another 1 h. In this step, the required amount of deionized water was added to the mixture to keep constant the volume of all dispersions (including the one with no added cellulose nanocrystals), taking as reference the nanocomposite containing 5 wt% of CNC (8.12 g), that is, the sample with the higher added water volume. The envisaged procedure is not expected to cause any instability effects in the Salvia-based dispersion since the pH of the used CNC suspension is above the critical isoelectric point value (~ 4.41) of the DMPA carboxylic groups. Nanocomposite films were prepared by casting the dispersions in Teflon molds, dried in a climatic chamber under controlled conditions (25 °C and 50 % of relative humidity) during 1 week. Subsequently, the films were further dried in a vacuum oven (25 °C) for 3 days sequentially at 800, 600 and 400 mbar. Nanocomposites were coded as WBPUU-X, where X (1, 3 or 5) is referred to the CNC content. A Salvia-based WBPUU film, i.e. a film without being added with CNC, was also prepared following the same dilution procedure, and denoted as WBPUU. A general scheme presenting the Salvia-based WBPUU synthesis, CNC isolation, and nanocomposites preparation and a table summarizing the samples codification, appearance and composition are shown in Fig. 1 and Table 1, respectively.

2.5. Characterization procedures

2.5.1. Cellulose nanocrystals

The concentration of sulfate groups anchored to the CNC surface during the hydrolysis process was determined by conductometric titration using a Crison EC-Meter GLP 31 conductometer calibrated with 147 μS/cm, 1413 μS/cm and 12.88 mS/cm standards. Titration measurements were done in triplicate at 25 °C using NaOH and HCl 10 mM. The sulfate concentration was also determined by elemental analysis using a Euro EA3000 Elemental Analyzer of Eurovector according to SCAB. PE.29.PR.10.02 method in the solid-state. Moreover, CNC were characterized by Fourier transform infrared spectroscopy and atomic force microscopy according to the methodologies described next in section 2.5.3.

2.5.2. Salvia-based WBPUU dispersion

Salvia-based WBPUU dispersion was characterized in terms of solids content (SC), pH, viscosity (η) and particle size.

Solids content was determined by the relation between the

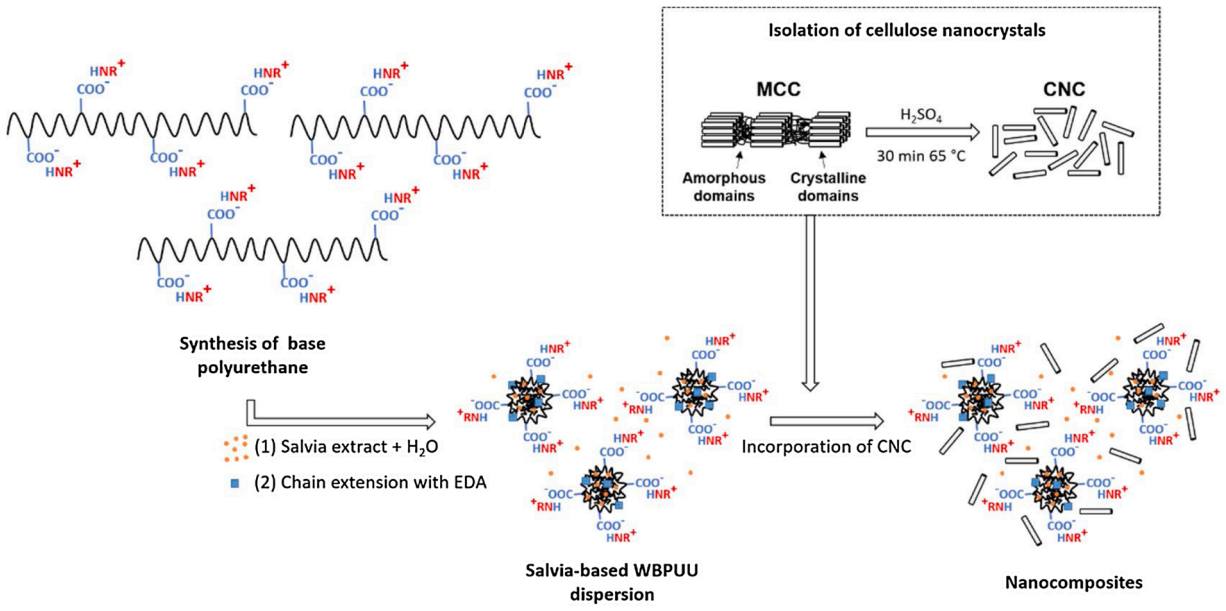

Fig. 1. General scheme of the nanocomposites preparation strategy.

Table 1
Codification, appearance and composition of the samples.

Sample codification	Appearance	CNC content (wt%)	General comments
Salvia-based WBPUU dispersion	Dispersion	0	**Polyurethane-urea dispersion composition** HS: 32 wt%; NCO/OH molar ratio 1.67; DBTDL: 0.037 wt %; DMPA: 5 wt%; EDA chain extension degree of 40%; Salvia content: 3 wt%
WBPUU	Film	0	
WBPUU-1	Film	1	
WBPUU-3	Film	3	
WBPUU-5	Film	5	

dispersion weight and the corresponding weight in its dry state. The weight of around 1 g of the dispersion before and after being dried for 1 h at 105 °C was measured by triplicate.

The pH was determined using a pH meter GLP22 of Crison calibrated with pH 4.00 and 7.00 buffer solutions standards.

The viscosity was measured in a Visco Star Fungilab of concentric cylinders rotational viscosimeter. Measurements were carried out by triplicate at 25 °C.

Particle size distribution was determined using a Mastersizer 3000 Hydro particle size analyzer of Malvern by averaging five replicates of the dispersion diluted in deionized water at 25 °C.

2.5.3. Nanocomposite and Salvia-based films

Nanocomposite Salvia-based film were characterized by Fourier transform infrared spectroscopy (FTIR), differential scanning calorimetry (DSC), mechanical analysis, and dynamic mechanical analysis (DMA). Moreover, morphology was analyzed by Atomic force microscopy (AFM).

Functional groups and hydrogen bonding interactions were analyzed by FTIR using a Nicolet Nexus spectrometer equipped with a MKII Golden Gate accessory (Specac) with a diamond crystal at a nominal incidence angle of 45° and ZnSe lens. Spectra were collected from 4000 to 650 cm^{-1} by averaging 64 scans with a resolution of 8 cm^{-1}.

The thermal behavior was analyzed by DSC using a Mettler Toledo 822e, equipped with a robotic arm and an intracooler. Between 5–10 mg were poured into aluminum pans and heated from −75 to 200 °C (20 °C/min) under nitrogen atmosphere. The glass transition temperature was ascribed as the inflexion point of the heat capacity change. For the endothermic peak, the maximum was considered the melting temperature and the area under the peak the melting enthalpy. Transitions were determined using a single measurement.

The mechanical behavior was accessed with a MTS insight 10 testing machine equipped with a 250 N load cell and pneumatic grips to hold samples, by averaging 5 specimens for each system. Films tensile modulus (E), maximum stress (σ_m), stress at break (σ_b) and strain at break (ε_b) were determined from the stress-strain curves obtained at a crosshead speed of 50 mm/min at room temperature. The break point (σ_b and ε_b) was settled as the sharp drop point at the end of the curve.

Thermomechanical properties were determined by dynamic mechanical analysis (DMA) using an Eplexor 100-N analyzer (Gabo) equipment. Films were measured in tensile mode, from -100 to 60 °C at a scan rate of 2 °C/min, with a static strain of 0.05 % and operating frequency of 1 Hz.

Morphology was analyzed by AFM using a Nanoscope IIIa scanning probe microscope (Multimode™ Digital Instruments) provided with an integrated force generated by cantilever/silicon probes (with a tip radius of 5–10 nm and 125 μm long), applying a resonance frequency of about 180 kHz. Samples were prepared by spin-coating a droplet of the dispersion on glass supports using a Spincoater P6700 at 2000 rpm for 130 s.

3. Results and discussion

3.1. Cellulose nanocrystals characterization

The isolation method of CNC by acid hydrolysis results in the anchoring of sulfate groups to the CNC surface, which favor the electrostatic repulsion forces between the formed nanoentities, promoting their dispersibility in polar solvents [13,15]. The anchoring degree was measured by conductimetric titration and elemental analysis resulting in values of 0.73 % and 0.70 %, respectively. These values are similar to other works [20] where it is reported that the range of sulfate anchoring percentage is usually between 0.66 and 1.1 %.

The successful isolation of CNC was evaluated by AFM, namely by inspecting the morphology and determining the length/diameter (L/D) aspect ratio. Fig. 2 shows the rod-like morphology of the CNC, presenting length and diameter in the nanoscale dimension. By averaging 100 CNC entities in the height profile and height image, length and diameter values of 167 ± 101 and 5.6 ± 1.5 nm, respectively, were

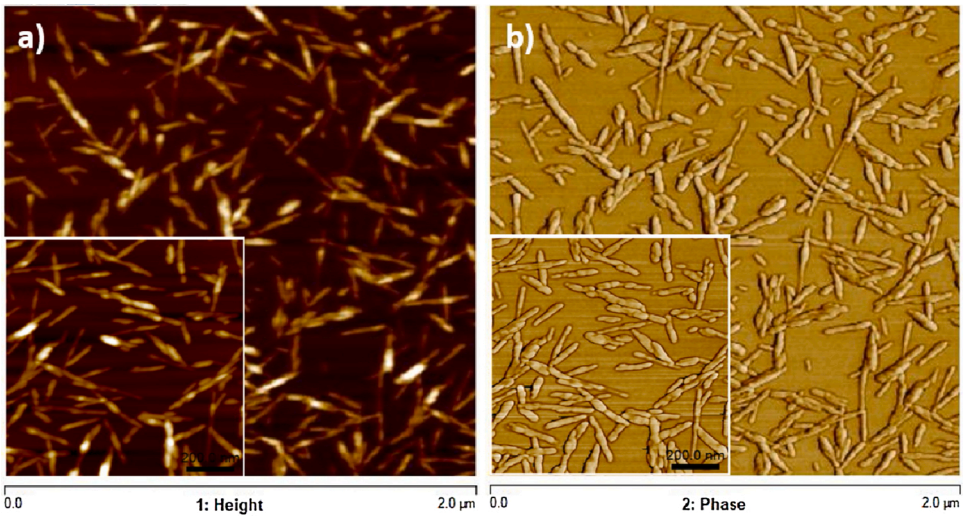

Fig. 2. AFM a) height and b) phase images of isolated CNC (2 µm) and inside, the corresponding amplification of 1 µm.

determined, resulting in a L/D aspect ratio of 30. The aspect ratio value is a key parameter determining the performance of the CNC in the nanocomposite [21]. The higher the value, greater reinforcing capacity will provide to the system. This value is in the upper range comparing with similar systems [20,22], availing the reinforcing effect it can transfer to prepared Salvia-based WBPUU nanocomposites.

3.2. Salvia-based WBPUU dispersion characterization

The solids content, pH and viscosity properties of the synthesized Salvia-based WBPUU dispersion and particle size distribution are shown in Fig. 3. The pH value of the dispersion around 7–8 is in the usual range on this type of dispersions, evidencing that carboxylic groups were effectively neutralized [23,24]. The SC value was around the theoretical value of the formulated dispersion while relative low viscosity was obtained. These values showed the suitability of the synthesis in face of its applicability, where high solids content and low viscosity values are usually preferred [25].

Regarding the particle size distribution, the dispersion resulted in a homogeneous and unimodal distribution, with an average particle size of 58.4 nm (deviation lower than 10^{-3}). The dispersion was visually stable over 6 months, fact related with the small particle size and the homogeneous distribution, that is known to favour dispersion's stability [26,27]. Furthermore, plant extracts can act as natural surfactants, favouring the formation of the small size and unimodal distribution of the nanoparticles, promoting the stability over time, as previously reported [9,28].

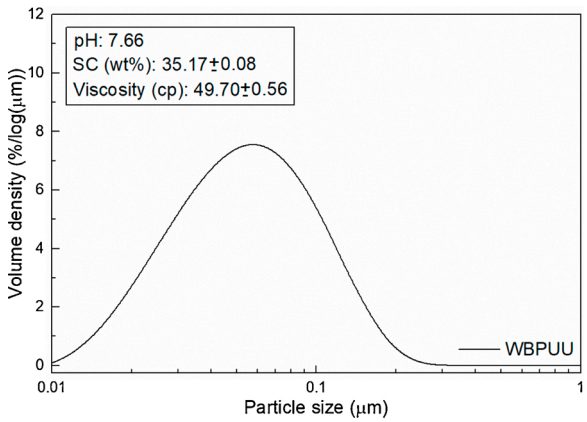

Fig. 3. Salvia-based WBPUU dispersion properties and particle size distribution in volume.

3.3. Nanocomposite and Salvia-based films characterization

The obtained Salvia-based film (WBPUU), and nanocomposite films (WBPUU-1, WBPUU-3 and WBPUU-5) are shown in Fig. 4. All films resulted transparent presenting a light brown colour. This fact would be related with the presence of the plant extracts compounds that have this colour hue.

Salvia-based WBPUU, nanocomposite films and CNC FTIR spectra are shown in Fig. 5. CNC spectrum showed the typical profile of cellulose [29]. Specifically, the broad band between 3000 and 3600 cm^{-1} correspond to the stretching vibration of hydrogen bonding and free hydroxyl groups whereas the band about 2900 cm^{-1} is related to the stretching vibration of CH groups. The slight band at about 1637 cm^{-1} is attributed to the water absorbed by CNC. Moreover, the fingerprint of cellulose is reflected by the bands corresponding to CH_2 symmetrical bending (1430 cm^{-1}), C—O—C stretching (1160 cm^{-1}), stretching of glucopyranose (1110 cm^{-1}) and β-glycosidic linkage vibration (895 cm^{-1}).

For Salvia-based WBPUU film, bands associated with different functional groups were observed. The band between 3000 and 3500 cm^{-1} was attributed to the N—H stretching vibration, and the two bands at 2947 and 2867 cm^{-1} to the stretching vibration of C—H groups. The band centred about 1720 cm^{-1} was associated with the stretching vibration of carbonyl (C═O) groups, the band at 1540 cm^{-1} with the C—N

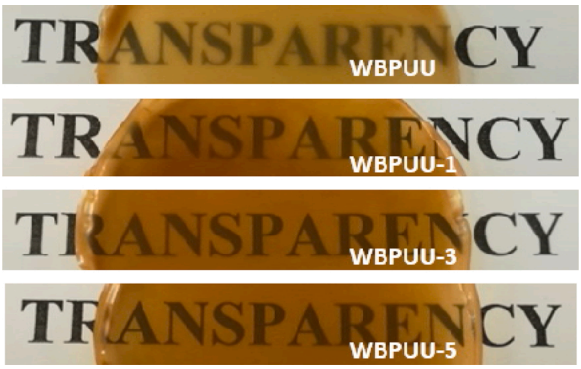

Fig. 4. Appearance of Salvia-based WBPUU matrix, and nanocomposite reinforced with CNC.

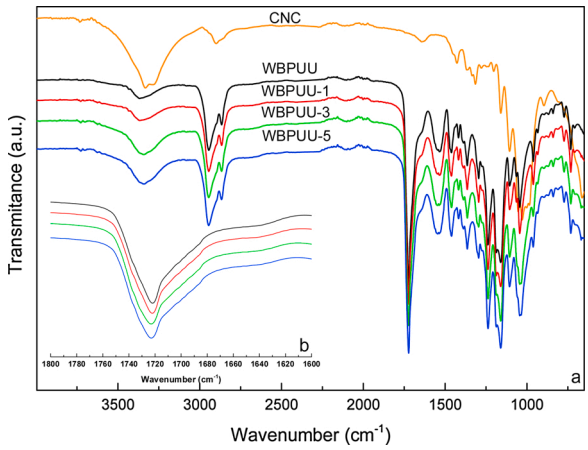

Fig. 5. a) FTIR spectra of CNC, Salvia-based WBPUU matrix and nanocomposites reinforced with CNC; b) amplification of carbonyl region.

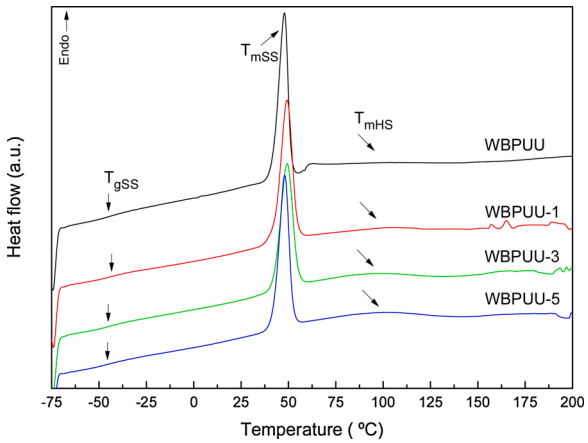

Fig. 6. DSC thermograms of Salvia-based WBPUU matrix and nanocomposites reinforced with CNC.

stretching vibration combined with N—H bending, and the bands located at 1460 and 1360 cm^{-1} with the asymmetric and symmetric bending vibration of C—H, respectively [30]. It should be noted the absence of the band at 2270 cm^{-1}, attributed to the isocyanate (NCO) groups, indicating that the dispersion synthesis procedure leaded to their complete conversion [31].

Analyzing the spectra of nanocomposites, the main variations occurred in the bands of N—H and C═O groups observed around 3000–3500 and 1800–1600 cm^{-1}, respectively. Regarding the N—H region, it is known that depending on the wavenumber the N—H groups can be associated with diverse structure and interactions. Bands centred about 3499 cm^{-1} are assigned to free N—H groups, and bands around 3372 and 3306 cm^{-1} correspond to N—H groups hydrogen-bonded to carbonyl (C═O) and ether oxygen groups (C—O—C), respectively [32]. In the case of the base WBPUU, the main peak centred around 3360 cm^{-1}, indicated that most of the N—H groups are involved in hydrogen bonds with carbonyl groups. The band increased as the CNC content increased, also shifting to lower wavenumber values (from 3360 to 3340 cm^{-1}), a fact that could be related with the hydrogen bonding generated between the N—H groups of the WBPUU matrix and the ether oxygen of CNC reinforcement. Similarly, in the C═O region, the nature of C═O groups, as well as their interactions, can result in different assignments. The deconvolution of the C═O region performed by Mishra and co-workers [32] for several systems, revealed that free C═O groups of both urethane and urea groups are located around 1740–1725 and 1725–1710 cm^{-1}, respectively, while hydrogen-bonded urethane and urea groups correspond to bands centred about 1685–1670 and 1655–1644 cm^{-1}, respectively.

Analyzing the spectra amplification provided in Fig. 5, the Salvia-based WBPUU presented a band around 1720 cm^{-1}corresponding to free C═O urethane groups (SS), broadening to lower wavenumbers pointing out the hydrogen bonding of C═O groups. Considering the nanocomposites with different CNC contents, their addition shifted and broadens the band at 1720 cm^{-1} to higher wavenumbers, suggesting that CNC addition led to a higher amount of urethane C═O free groups. Moreover, the shoulder intensity increase, by broadening to lower wavenumber values, indicated that the C═O involved in hydrogen bonds were also increased.

The thermal behaviour of the Salvia-based WBPUU and nanocomposites was analyzed by DSC, and the thermograms and transition values are shown in Fig. 6 and Table 2, respectively.

Salvia-based WBUU matrix and nanocomposites showed different transitions associated with both soft and hard domains. In the Salvia-based WBPUU matrix, the glass transition (−45 °C), associated with the mobility of the soft domain (T_{gSS}) was determined setting the baseline between the start and end temperatures of −59 and −28 °C, respectively. Moreover, a sharp endothermic peak associated with the ordered soft domains (47.7 °C), and a slight endothermic transition at 101.5 °C, attributable to the short range ordered hard domains, are shown (determined setting the baseline between the start and end temperature ranges of 33 and 56 °C, and 68 and 135 °C, respectively).

Table 2
Thermal properties of Salvia-based WBPUU matrix and nanocomposites reinforced with CNC.

Sample	T_{gSS}(°C)	T_{mSS} (°C)	ΔH_{mSS} (J/g)	T_{mHS} (°C)	ΔH_{mHS} (J/g)
WBPUU	−45.0	47.7	30.2	101.5	0.9
WBPUU-1	−43.0	49.3	31.1	102.5	3.6
WBPUU-3	−45.0	49.3	28.7	95.1	5.6
WBPUU-5	−45.7	47.9	29.5	99.4	7.0

In general, the CNC incorporation leads to the maintenance of the transitions observed in the matrix. However, some differences were noticed indicating that CNC presence modified the base structure assumed by the matrix during the film formation. Attending to the T_{gSS} of the soft domain, at low CNC content (1 wt%), a slight increase in this temperature was observed, in comparison with the WBPUU matrix. This fact implies that the restriction in the mobility of the soft amorphous domain, due to the addition of 1 wt% of CNC, but leading to a progressive decrease in the T_{gSS} by higher CNC addition thus suggesting a greater mobility of this domain, indicating that could not be strongly associated with CNC by hydrogen bonds [30]. This fact was previously suggested by the FTIR analysis where the peak at 1720 cm^{-1} associated to free C═O groups broadened and shifted to higher wavenumbers as the incorporated CNC content increased.

Regarding soft and hard ordered domains, more remarkable changes were observed. The presence of both transitions indicate that the Salvia-based WBPUU matrix structure presented phase separation, which is enhanced with CNC incorporation, resulting in a progressive increase in the ordering capacity of the hard domains, which became segregated from the soft domain, showing higher ΔH_{mHS} values. Moreover, the increasingly ordered hard domains can influence the arrangement capacity of the soft domain, considering that a higher order degree of the hard domain hinders the crystallization ability of the soft domain [33], leading to slightly lower ΔH_{mSS} values. Furthermore, the higher segregated phase structure of samples WBUU-1 and WBUU-3, compatible with the observed higher T_{mSS} value, can be related with the formation of more ordered crystals. Concretely, it should be noted that in WBPUU-1, the increase of both ordered domains in terms of quantity (higher ΔH_{mSS} and ΔH_{mHS}) and packaging level (higher T_{mSS} and T_{mHS}), resulted in the registered increase in T_{gSS} value, due to restrictions to chain mobility [27].

The mechanical behaviour of Salvia-based WBPUU matrix and nanocomposites are shown in Fig. 7, and the mechanical properties are summarized in Table 3.

Results showed that the incorporation of CNC was effective up 5 wt% load, leading to a suitable stress-transfer between the matrix and the reinforcement, translated by a progressive increase in E and σ_{max} values [34], objective pursued in this work. Indeed, sample WBUU-5 almost duplicates E value, comparatively with the matrix. Usually, the addition of CNC results in a stiffening effect of the film [35,36], evidenced by a decrease in strain at break values due to the high rigidity of cellulose [37]. In this study, this common effect was observed in the case of the composite with 1 wt% CNC (WBUU-1), where strain at break decreased in comparison with the Salvia-based WBPUU matrix. Appositively, the incorporation of 3 and 5 wt% CNC led to slight increase of the strain at break value, being possible influenced by alternative effects including the domains distribution adopted by the Salvia-based WBPUU, as previously discussed in DSC results section. The elongation capacity could be conditioned mainly by the mobility of the amorphous chains, that is, the SS, considering the increase of hard domains order (which should be reflected in more rigid films, fact not observed in the studied system). When using 1 wt% CNC composite, where higher ΔH_{mSS} and T_{mSS} were observed, along with T_{gSS} increase, a reduction in strain at break value was registered. However, in the composites using 3 and 5 wt% CNC, the strain at break was maintained in comparison with the one of the Salvia-based WBPUU matrix, where less ordered soft domains were observed (lower ΔH_{mSS} and T_{gSS}), suggesting a higher freedom of the soft chains (enhanced flexibility).

It should be worth noting that the Salvia-based WBPUU film led to different mechanical properties in comparison with the analogous system previously reported [9]. The direct casting of the Salvia-based dispersions resulted in films with higher flexibility (847 %) and lower stiffness (E of 4.5 MPa), whereas for the films produced in the present work values of 41 % and 333.1 MPa, respectively, were obtained. In fact, the used dilution step influenced the drying conditions of the films, originating different organization structures and thus different properties (e.g. thermal and mechanical), as also previously reported in the literature. Tapia-Blácido et al. [38] demonstrated the effect of temperature and relative humidity in the drying rate, which have influenced the mechanical properties of amaranth flour films with glycerol as plasticizer; namely, low drying rates, originated films with higher E values. Kundu et al. [39], analyzed the influence of film preparation procedures on crystallinity, morphology and mechanical properties of linear low-density polyethylene added with calcite filler, revealing that the processing as well as the cooling conditions led to materials with elongation values ranging from 63 to 573 %.

The thermomechanical behaviour of Salvia-based WBPUU matrix and nanocomposites was determined by DMA. The storage modulus (E') and Tanδ curves are shown in Fig. 8. The glassy-state, observed in the range −100 to −50 °C, was characterized for maintaining E' almost constant, independently of the used CNC content, due to chains mobility hindrance. At higher temperatures, a decrease in the E' was observed, usually reflected by a peak in Tanδ curves. This transition is associated with the material's T_g [26]. In this case, a pronounced shoulder was observed from −50 to −20 °C, in accordance with the T_{gSS} values obtained by DSC. Below the T_{gSS} transition, it was observed that the prepared nanocomposites showed slightly lower E' values in comparison with the Salvia-based WBPUU matrix, being progressively higher as the CNC content increases. This fact indicates that the CNC reinforcing effect would not be directly related to their interaction with the soft segment [27], as previously discussed in DSC results. By contrast, at higher temperatures, which would be related to the hard ordered domains, interaction effects occurred. In this region, it was observed that the E' curves obtained for nanocomposites, including the one with 1 wt% CNC, exceeded the one of the Salvia-based WBPUU matrix, reflecting an enhancement of the thermomechanical stability of this film, which is progressively improved with the increase of CNC content. This reinforcing effect suggests that CNC interacts with the hard segment at a greater extent that together with the formed more ordered domains, would favour the retard of the flow point of the nanocomposites [36].

The morphology of Salvia-based WBPU matrix and CNC nanocomposites was analyzed by AFM, and height and phase images are shown in Fig. 9. It is known that in general, the dark regions are associated with the soft segment, whereas bright regions are related to hard domains [40]. Attending to the Salvia-based WBPUU matrix, it was observed a spherical and homogeneous distribution that could be related with the coalescence of WBPUU dispersion nanoparticles, which present high film-forming ability. The typical core-shell structure adopted by the dispersion nanoparticles where the hydrophobic segment (SS) forms the core and the hydrophilic segment (HS) arranges to form the shell, leads to the observed structure conformed by dark spheres surrounded by a bright cover. Furthermore, it should be worth noting that CNC addition

Table 3
Mechanical properties of Salvia-based WBPUU matrix and nanocomposites reinforced with CNC.

Sample	Modulus (MPa)	Maximum stress (MPa)	Stress at break (MPa)	Strain at break (%)
WBPUU	333.1 ± 13.4	10.4 ± 0.4	4.5 ± 0.9	41 ± 8
WBPUU-1	398.9 ± 3.9	10.7 ± 0.5	3.5 ± 1.5	30 ± 7
WBPUU-3	452.5 ± 10.6	10.8 ± 0.8	3.0 ± 1.1	39 ± 9
WBPUU-5	523.6 ± 15.8	11.8 ± 0.6	3.6 ± 0.9	45 ± 5

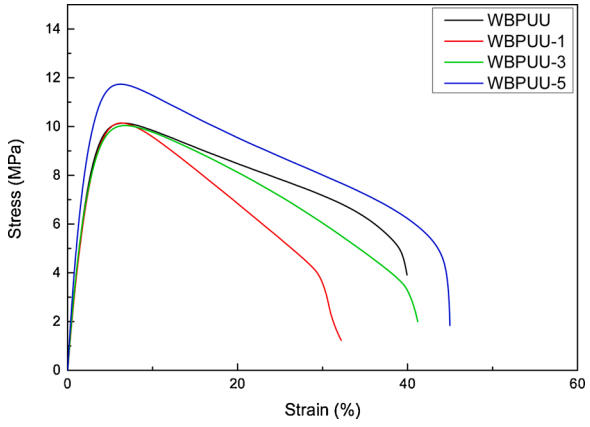

Fig. 7. Stress-strain curves of Salvia-based WBPUU matrix and nanocomposites reinforced with CNC.

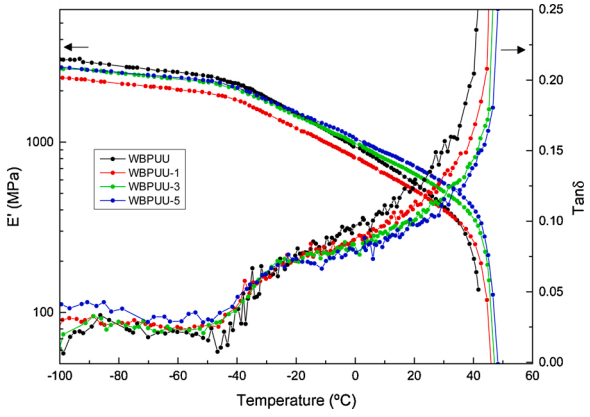

Fig. 8. E' and Tanδ curves of Salvia-based WBPUU matrix and nanocomposites reinforced with CNC.

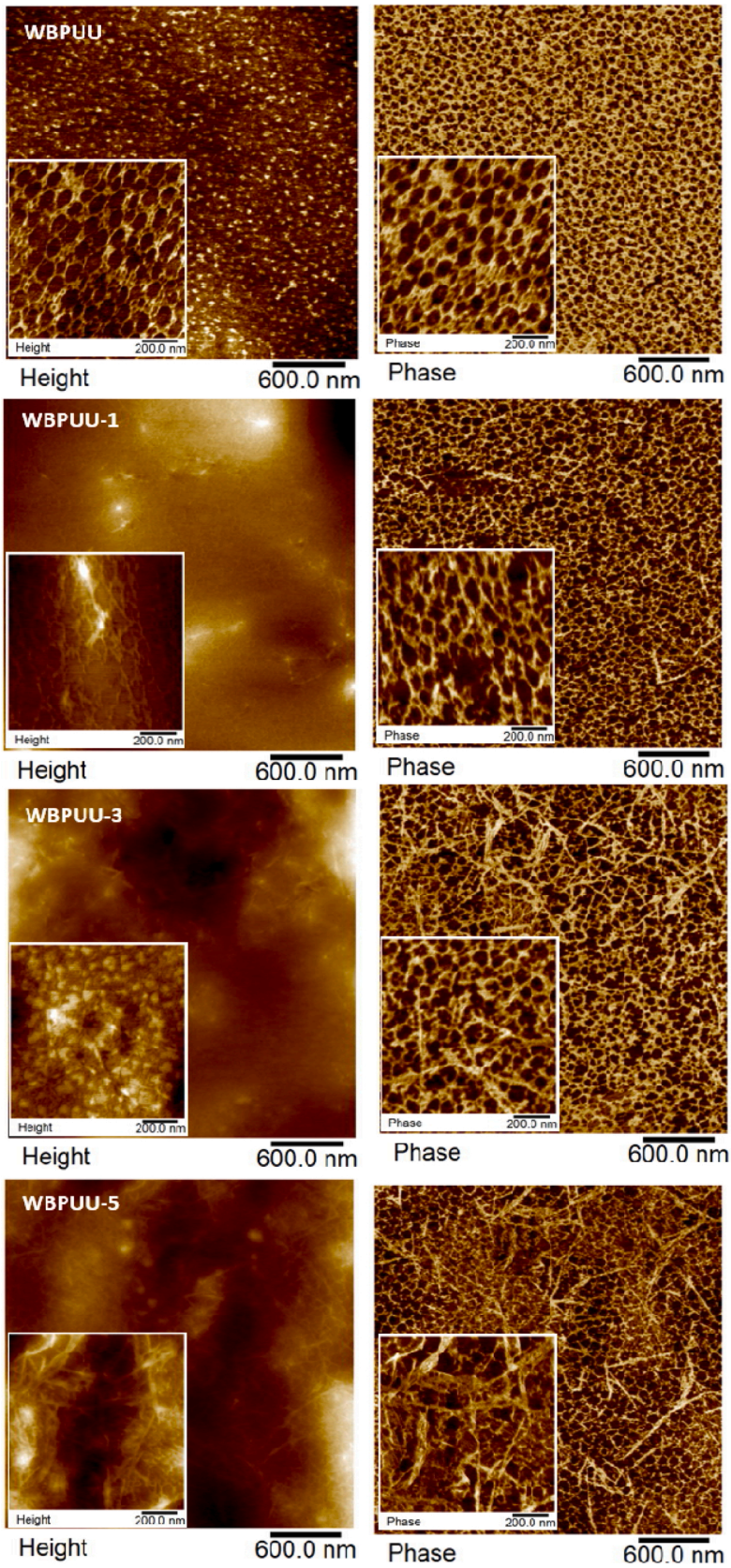

Fig. 9. AFM tapping mode height (left) and phase (right) images of Salvia-based WBPUU matrix and nanocomposites of 3 μm and inside, the corresponding amplification of 1 μm.

maintains, in general, the spherical morphology. In particular, in CNC nanocomposite images, the bright appearance of CNC indicates the stiff character of the nanoreinforcement, whose significant presence, according to the increased addition of CNC content, corroborates their effective loading into the nanocomposites. Moreover, for all the tested samples, CNC were uniformly distributed, availing the absence of agglomerates formation during the film-forming process [36], which might favour stress-transfer, as previously addressed in the mechanical properties section.

4. Conclusions

In this work, a Salvia-based WBPUU dispersion loaded with 3 wt% of Salvia extract during the inversion phase was synthesized. DLS results showed the low and narrow particle size distribution of the Salvia-based WBPUU dispersion, which can be ascribed to the effective synthesis method favored by the natural extract surfactant. The dispersion was used in the preparation of green nanocomposites by the incorporation of isolated high L/D aspect ratio (30) CNC, whose homogeneous distribution was corroborated by AFM. FTIR results revealed the addition of CNC led to the increase of both, free C═O groups in the SS and hydrogen bonded C═O groups in the HS. DSC results pointed out a reorganization of the phases induced by CNC incorporation, that, in general, resulted in lower T_{gSS} values (indicating the increased mobility of the amorphous fraction of soft domains), while promoting the arrangement of short range ordered hard domains, evidenced by the increase of ΔH_{mHS} values. The structure adopted by the WBPUU, together with the stiff CNC, lead to composites with enhanced mechanical properties (higher E), and increased elongation capacity. Similarly, the thermomechanical behaviour was improved, retarding the flow temperature to higher values.

CRediT authorship contribution statement

Arantzazu Santamaria-Echart: Conceptualization, Data curation, Investigation, Methodology, Resources, Supervision, Validation, Visualization, Writing - original draft, Writing - review & editing. **Isabel Fernandes:** Data curation, Investigation, Methodology, Resources. **Lorena Ugarte:** Data curation, Investigation, Methodology, Resources. **Filomena Barreiro:** Conceptualization, Funding acquisition, Project administration, Writing - original draft, Writing - review & editing. **Maria Angeles Corcuera:** Conceptualization, Funding acquisition, Supervision, Visualization, Writing - original draft, Writing - review & editing. **Arantxa Eceiza:** Conceptualization, Funding acquisition, Project administration, Supervision, Visualization, Writing - original draft, Writing - review & editing.

Declaration of Competing Interest

The authors declare that they have no known competing financial interests or personal relationships that could have appeared to influence the work reported in this paper.

Acknowledgements

Financial support from the University of the Basque Country (UPV/EHU) (GIU18/216 Research Group), the Spanish Ministry of Economy and Competitiveness (MINECO) (MAT2016-76294-R). Foundation for Science and Technology (FCT, Portugal) for financial support by national funds FCT/MCTES to CIMO (UIDB/00690/2020). National funding by FCT- Foundation for Science and Technology, through the institutional scientific employment program-contract with I.P. Fernandes. We also wish to acknowledge the "Macrobehaviour-Mesostructure-Nanotechnology" SGIker units from the UPV/EHU, for their technical support. A.S-E thanks the UPV/EHU for the Ph.D. grant (PIF/UPV/12/201).

References

[1] A.C. Ospina, V.H. Orozco, L.F. Giraldo, M. Fuensanta, J.M. Martín-Martínez, N. Mateo-Oliveras, Study of waterborne polyurethane materials under aging treatments, Effect of the soft segment length, Prog. Org. Coatings. 138 (2020), https://doi.org/10.1016/j.porgcoat.2019.105357, 105357.
[2] S. Saalah, L.C. Abdullah, M.M. Aung, M.Z. Salleh, D.R. Awang Biak, M. Basri, E. R. Jusoh, Waterborne polyurethane dispersions synthesized from jatropha oil, Ind. Crops Prod. 64 (2015) 194–200, https://doi.org/10.1016/j.indcrop.2014.10.046.
[3] Z. Yang, G. Wu, Effects of soft segment characteristics on the properties of biodegradable amphiphilic waterborne polyurethane prepared by a green process, J. Mater. Sci. 55 (2020) 3139–3156, https://doi.org/10.1007/s10853-019-04237-6.
[4] Y. Zhang, W. Zhang, X. Wang, Q. Dong, X. Zeng, R.L. Quirino, Q. Lu, Q. Wang, C. Zhang, Waterborne polyurethanes from castor oil-based polyols for next generation of environmentally-friendly hair-styling agents, Prog. Org. Coatings. 142 (2020), https://doi.org/10.1016/j.porgcoat.2020.105588, 105588.
[5] T. Xie, W. Kao, L. Sun, J. Wang, G. Dai, Z. Li, Preparation and characterization of self-matting waterborne polymer–An overview, Prog. Org. Coatings. 142 (2020), 105569, https://doi.org/10.1016/j.porgcoat.2020.105569.
[6] E. Shin, S. Choi, J. Lee, Fabrication of regenerated cellulose nanoparticles/waterborne polyurethane nanocomposites, J. Appl. Polym. Sci. 135 (2018), https://doi.org/10.1002/app.46633, 46633/1-46633/8.
[7] C. Sharma, N.K. Bhardwaj, Fabrication of natural-origin antibacterial nanocellulose films using bio-extracts for potential use in biomedical industry, Int. J. Biol. Macromol. 145 (2020) 914–925, https://doi.org/10.1016/j.ijbiomac.2019.09.182.
[8] T.D. Tavares, J.C. Antunes, F. Ferreira, H.P. Felgueiras, Biofunctionalization of natural fiber-reinforced biocomposites for biomedical applications, Biomolecules. 10 (2020) 1–44, https://doi.org/10.3390/biom10010148.
[9] A. Santamaria-Echart, I. Fernandes, F. Barreiro, A. Retegi, A. Arbelaiz, M. A. Corcuera, A. Eceiza, Development of waterborne polyurethane-ureas added with plant extracts: study of different incorporaton routes and their influence on particle size, thermal, mechanical and antibacterial properties, Prog. Org. Coatings. 117 (2018) 76–90.
[10] C. Tober, R. Schoop, Modulation of neurological pathways by Salvia officinalis and its dependence on manufacturing process and plant parts used, BMC Complement, Altern. Med. 19 (2019) 1–10, https://doi.org/10.1186/s12906-019-2549-x.
[11] F.T. Seta, X. An, L. Liu, H. Zhang, J. Yang, W. Zhang, S. Nie, S. Yao, H. Cao, Q. Xu, Y. Bu, H. Liu, Preparation and characterization of high yield cellulose nanocrystals (CNC) derived from ball mill pretreatment and maleic acid hydrolysis, Carbohydr. Polym. 234 (2020), 115942, https://doi.org/10.1016/j.carbpol.2020.115942.
[12] H. Doh, M.H. Lee, W.S. Whiteside, Physicochemical characteristics of cellulose nanocrystals isolated from seaweed biomass, Food Hydrocoll. 102 (2020), 105542, https://doi.org/10.1016/j.foodhyd.2019.105542.
[13] A. Santamaria-Echart, L. Ugarte, A. Arbelaiz, N. Gabilondo, M.A. Corcuera, A. Eceiza, Two different incorporation routes of cellulose nanocrystals in waterborne polyurethane nanocomposites, Eur. Polym. J. 76 (2016) 99–109, https://doi.org/10.1016/j.eurpolymj.2016.01.035.
[14] A. Santamaria-Echart, L. Ugarte, A. Arbelaiz, F. Barreiro, M.A. Corcuera, A. Eceiza, Modulating the microstructure of waterborne polyurethanes for preparation of environmentally friendly nanocomposites by incorporating cellulose nanocrystals, Cellulose. 24 (2017) 823–834, https://doi.org/10.1007/s10570-016-1158-9.
[15] A. Santamaria-Echart, L. Ugarte, C. García-Astrain, A. Arbelaiz, M.A. Corcuera, A. Eceiza, Cellulose nanocrystals reinforced environmentally-friendly waterborne polyurethane nanocomposites, Carbohydr. Polym. 151 (2016) 1203–1209.
[16] A. Santamaria-Echart, L. Ugarte, K. Gonzalez, L. Martin, L. Irusta, A. Gonzalez, M. A. Corcuera, A. Eceiza, The role of cellulose nanocrystals incorporation route in waterborne polyurethane for preparation of electrospun nanocomposites mats, Carbohydr. Polym. 166 (2017) 146–155, https://doi.org/10.1016/j.carbpol.2017.02.073.
[17] A. Santamaria-Echart, I. Fernandes, L. Ugarte, F. Barreiro, A. Arbelaiz, M. Angeles, A. Eceiza, Waterborne polyurethane-urea dispersion with chain extension step in homogeneous medium reinforced with cellulose nanocrystals, Compos. Part B Eng. 137 (2018) 31–38.
[18] M. Nasrollahzadeh, M. Sajjadi, J. Dadashi, H. Ghafuri, Pd-based nanoparticles: plant-assisted biosynthesis, characterization, mechanism, stability, catalytic and antimicrobial activities, Adv. Colloid Interface Sci. 276 (2020), 102103, https://doi.org/10.1016/j.cis.2020.102103.
[19] I. Nowrouzi, A.H. Mohammadi, A.K. Manshad, Water-oil interfacial tension (IFT) reduction and wettability alteration in surfactant flooding process using extracted saponin from Anabasis Setifera plant, J. Pet. Sci. Eng. 189 (2020), 106901, https://doi.org/10.1016/j.petrol.2019.106901.
[20] M.S. Reid, M. Villalobos, E.D. Cranston, Benchmarking cellulose nanocrystals: from the laboratory to industrial production, Langmuir. 33 (2017) 1583–1598, https://doi.org/10.1021/acs.langmuir.6b03765.
[21] Q. Wu, X. Li, Q. Li, S. Wang, Y. Luo, Estimation of aspect ratio of cellulose nanocrystals by viscosity measurement: Influence of aspect ratio distribution and ionic strength, Polymers (Basel). 11 (2019) 1–12, https://doi.org/10.3390/polym11050781.
[22] I.A. Sacui, R.C. Nieuwendaal, D.J. Burnett, S.J. Stranick, M. Jorfi, C. Weder, E. J. Foster, R.T. Olsson, J.W. Gilman, Comparison of the properties of cellulose nanocrystals and cellulose nanofibrils isolated from bacteria, tunicate, and wood processed using acid, enzymatic, mechanical, and oxidative methods, ACS Appl, Mater. Interfaces. 6 (2014) 6127–6138, https://doi.org/10.1021/am500359f.

[23] G.P. Lokhande, S.U. Chambhare, R.N. Jagtap, Anionic water-based polyurethane dispersions for antimicrobial coating application, Polym. Bull. Berl. (Berl) 74 (2017) 4781–4798, https://doi.org/10.1007/s00289-017-1965-7.
[24] V. García-Pacios, Y. Iwata, M. Colera, J. Miguel Martín-Martínez, Influence of the solids content on the properties of waterborne polyurethane dispersions obtained with polycarbonate of hexanediol, Int. J. Adhes. Adhes. 31 (2011) 787–794, https://doi.org/10.1016/j.ijadhadh.2011.05.010.
[25] X. mei Wang, Q. Li, A new method for preparing low viscosity and high solid content waterborne polyurethane-Phase inversion research, Prog. Org. Coatings. 131 (2019) 285–290, https://doi.org/10.1016/j.porgcoat.2019.02.001.
[26] H. Liang, L. Liu, J. Lu, M. Chen, C. Zhang, Castor oil-based cationic waterborne polyurethane dispersions: storage stability, thermo-physical properties and antibacterial properties, Ind. Crops Prod. 117 (2018) 169–178, https://doi.org/10.1016/j.indcrop.2018.02.084.
[27] W. Lei, X. Zhou, C. Fang, Y. Song, Y. Li, Eco-friendly waterborne polyurethane reinforced with cellulose nanocrystal from office waste paper by two different methods, Carbohydr. Polym. 209 (2019) 299–309, https://doi.org/10.1016/j.carbpol.2019.01.013.
[28] S.T. Muntaha, M.N. Khan, Natural surfactant extracted from Sapindus mukurossi as an eco-friendly alternate to synthetic surfactant - a dye surfactant interaction study, J. Clean. Prod. 93 (2015) 145–150, https://doi.org/10.1016/j.jclepro.2015.01.023.
[29] K. Sahlin, L. Forsgren, T. Moberg, D. Bernin, M. Rigdahl, G. Westman, Surface treatment of cellulose nanocrystals (CNC): effects on dispersion rheology, Cellulose. 25 (2018) 331–345, https://doi.org/10.1007/s10570-017-1582-5.
[30] M.S. Kim, K.M. Ryu, S.H. Lee, Y.C. Choi, Y.G. Jeong, Influences of cellulose nanofibril on microstructures and physical properties of waterborne polyurethane-based nanocomposite films, Carbohydr. Polym. 225 (2019), 115233, https://doi.org/10.1016/j.carbpol.2019.115233.
[31] L. Man, Y. Feng, Y. Hu, T. Yuan, Z. Yang, A renewable and multifunctional eco-friendly coating from novel tung oil-based cationic waterborne polyurethane dispersions, J. Clean. Prod. 241 (2019), 118341, https://doi.org/10.1016/j.jclepro.2019.118341.
[32] A.K. Mishra, D.K. Chattopadhyay, B. Sreedhar, K.V.S.N. Raju, FT-IR and XPS studies of polyurethane-urea-imide coatings, Prog. Org. Coatings. 55 (2006) 231–243, https://doi.org/10.1016/j.porgcoat.2005.11.007.
[33] Y. Xiao, L. Jiang, Z. Liu, Y. Yuan, P. Yan, C. Zhou, J. Lei, Effect of phase separation on the crystallization of soft segments of green waterborne polyurethanes, Polym. Test. 60 (2017) 160–165.
[34] G. Dias, M. Prado, C. Le Roux, M. Poirier, P. Micoud, R. Ligabue, F. Martin, S. Einloft, Synthetic talc as catalyst and filler for waterborne polyurethane-based nanocomposite synthesis, Polym. Bull. Berl. (Berl) 77 (2020) 975–987, https://doi.org/10.1007/s00289-019-02789-w.
[35] R. De Chen, C.F. Huang, S. hui Hsu, Composites of waterborne polyurethane and cellulose nanofibers for 3D printing and bioapplications, Carbohydr. Polym. 212 (2019) 75–88, https://doi.org/10.1016/j.carbpol.2019.02.025.
[36] D. Cheng, P. Wei, L. Zhang, J. Cai, New approach for the fabrication of carboxymethyl cellulose nanofibrils and the reinforcement effect in water-borne polyurethane, ACS Sustain. Chem. Eng. 7 (2019) 11850–11860, https://doi.org/10.1021/acssuschemeng.9b02424.
[37] G. Josefsson, F. Berthold, E.K. Gamstedt, Stiffness contribution of cellulose nanofibrils to composite materials, Int. J. Solids Struct. 51 (2014) 945–953, https://doi.org/10.1016/j.ijsolstr.2013.11.018.
[38] D.R. Tapia-Blácido, P.Jd.A. Sobral, F.C. Menegalli, Effect of drying conditions and plasticizer type on some physical and mechanical properties of amaranth flour films, LWT - Food Sci. Technol. 50 (2013) 392–400, https://doi.org/10.1016/j.lwt.2012.09.008.
[39] P.P. Kundu, J. Biswas, H. Kim, S. Choe, Influence of film preparation procedures on the crystallinity, morphology and mechanical properties of LLDPE films, Eur. Polym. J. 39 (2003) 1585–1593, https://doi.org/10.1016/S0014-3057(03)00056-9.
[40] C. Tian, S.Y. Fu, Q.J. Meng, L.A. Lucia, New insights into the material chemistry of polycaprolactone-grafted cellulose nanofibrils/polyurethane nanocomposites, Cellulose. 23 (2016) 2457–2473, https://doi.org/10.1007/s10570-016-0980-4.